

## NUMERICAL EVALUATION OF LIGHTWEIGHT AGGREGATE CONCRETE MECHANICAL PROPERTIES

Aldemon BONIFÁCIO <sup>a</sup>, Julia MENDES <sup>b</sup>, Flávio BARBOSA <sup>c</sup>, Michèle FARAGE <sup>d\*</sup>,  
Sophie ORTOLA<sup>e</sup>, Fernanda MOREIRA <sup>f</sup>

<sup>a</sup> PhD student in Computational Modeling; Federal University of Juiz de Fora, Brazil

<sup>b</sup> MSc Student in Civil Engineering; Federal University of Ouro Preto, Brazil

<sup>c</sup> Associate Prof.; Federal University of Juiz de Fora, Brazil

<sup>d</sup> Associate Prof.; Federal University of Juiz de Fora, Brazil  
E-mail address: *michele.farage@ufff.edu.br*

<sup>e</sup> Dr. Eng.; Mechanics, University of Cergy-Pontoise, France

<sup>f</sup> Undergraduate Student in Civil Engineering; Federal University of Juiz de Fora, Brazil

Received: 26.03.2015; Revised: 11.05.2015; Accepted: 29.06.2015

### Abstract

The compressive behaviour of Lightweight Aggregate Concrete (LWAC) specimens was simulated through the Finite Element Method (FEM). The specimens were modelled so as to reproduce experimental data available in the literature. The numerical model considered the material as biphasic, composed of mortar – for which the mechanical properties were experimentally measured – and expanded clay – analytically characterized in a previous work. Numerical results showed fair agreement with experimental data, encouraging further applications with a higher level of complexity concerning geometrical and mechanical aspects.

### Streszczenie

Zachowanie na ściskanie próbek z betonu lekkiego kruszywowego (LWAC) zostało zamodelowane przy użyciu metody elementów skończonych (MES). Próbki były modelowane tak, aby odtworzyć dane doświadczalne, dostępne w literaturze. W modelu założono materiał dwufazowy, składający się z zaprawy – którego właściwości mechaniczne zostały wyznaczone eksperymentalnie – i glina – scharakteryzowany analitycznie w poprzedniej pracy. Wyniki numeryczne wykazały dobrą zgodność z danymi doświadczalnymi, zachęcając do dalszych zastosowań na wyższym poziomie złożoności dotyczących aspektów geometrycznych i mechanicznych.

Keywords: Concrete; FEM analysis; Lightweight aggregates; Mechanics of materials; Numerical modelling.

## 1. INTRODUCTION

Lightweight Aggregate Concrete (LWAC) is a versatile material that has been used in civil and naval construction worldwide for decades. Some of its main advantages over Normal-weight Aggregate Concrete (NWAC) are: reduced dead load due to low self-

weight, better thermal and acoustic insulation, and improved fire resistance, which may lead to a reduction in the overall cost of project. The use of LWAC allows for reduced sections on structural elements, larger spans, decreased amount of required steel, and therefore can be economically and efficiently applied to several types of buildings.

Although LWAC presents reduced weight and thus a structural advantage, its mechanical resistance is in general lower than that of ordinary concretes. In spite of this fact, the material is employed in civil construction in structural (load bearing) and non-structural elements. The examples below illustrate its efficiency when applied to high-rise construction. The One Shell Plaza Tower, a 220 m office building in Houston, has all its structural elements incorporating lightweight aggregates (Fig. 1). In turn, the Barclays Bank Head Office, located in Canary Wharf, London, is an example of mixed construction techniques – its structure is based on steel frame, whereas the slabs are built with composite deck slabs of lightweight aggregate concrete (Fig. 2). In both cases, LWAC was used as a form of reducing the weight of the elements, improving room insulation, besides adding hours of fire resistance with no extra measure, allying economical and safety advantages.

Differently from NWACs, where the aggregate is more resistant than the mortar and cracking begins in the interfacial transition zone (ITZ), in LWACs the weakest phase is the aggregate – which has a strong influence on the concrete's properties [2]. Fig. 3 shows the aspect of expanded clay grains while Fig. 4 illustrates the longitudinal section of a cylindrical sample made of LWAC.

For practical design purposes, it is convenient to be able to estimate the mechanical properties of hardened concrete based on its composition. Concerning LWAC's, though, this is a rather complex task due to the fact that the mechanical properties of LWAs are not easily measured through experimental techniques. Amongst the methods currently employed to evaluate LWA's compressive strength are experimental procedures and empirical correlations to its bulk density. The standard experimental method is the aggregate crushing test, which records the required pressure for the specimen to reach a 20 mm or 50 mm compression by means of a hydraulic press (BS EN 13055-1:2003) [4]. The resultant compressive strength of the aggregate from the crush test ( $f_{a,exp}$ ), however, does not accurately reflect the failure mode of the LWA in the concrete [5]; thus impairing the prediction of the LWAC compressive strength. In turn, empirical equations that relate the compressive strength to bulk densities fail to consider inherent characteristics of the aggregate (i.e. composition, origin, storage conditions, handling) and hence are not considered as reliable options for the material's characterization.

In the previous work, *Ke et al.* [5] employed an analytical inverse method for estimating the compressive



Figure 1.  
One Shell Plaza Tower, Houston, USA [1]



Figure 2.  
Barclays Bank Head Office, London, UK (photo by Simon Judd)

strength of LWAs ( $f_a$ ). Through a micromechanical scheme, the authors managed to obtain that property from experimental compressive strengths ( $f_c$ ) measured on LWAC samples. The adopted input parameters were: Compressive strength ( $f_m$ ) and Young modulus ( $E_m$ ) of the mortar matrix (experimentally obtained), volume fraction of LWA adopted in the concrete's mixture, compressive strength measured on hardened LWAC specimens ( $f_c$ ) and Young modulus of the LWA ( $E_a$ ), evaluated with Eq. (1):

$$E_a = 8000\rho_{ard}^2 \quad (1)$$

where  $\rho_{ard}$  is the dry density of the lightweight aggregate [5].



**Figure 3.**  
Lightweight Aggregate – Expanded Clay (picture: public domain)

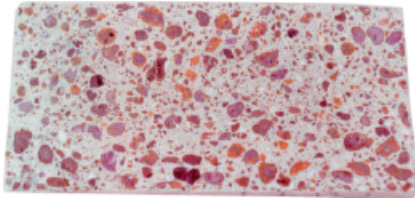


**Figure 4.**  
Longitudinal section of a LWAC specimen [3]

By adopting the aggregate and the mortar properties –  $f_a$ ,  $E_a$ ,  $f_m$  and  $E_m$  – experimentally and/or analytically measured – the present study simulates the behaviour of LWAC specimens when subjected to compressive load. To this end, it is employed the free Finite Element (FE) code Cast3M, developed by the French Atomic Energy and Alternative Energies Commission (Commissariat à l'Énergie Atomique et aux Énergies Alternatives, CEA). The output of the numerical analysis is an estimate of the compressive strength ( $f_c$ ) of the LWAC. For validation purposes, the numerical data are compared to the results of an experimental program where the  $f_{c,exp}$  of LWAC cylindrical specimens was measured via mechanical tests.

## 2. NUMERICAL PROGRAM

### 2.1. Overall Description

The numerical program described herein was accomplished through Cast3M. This software applies the Finite Element Method to several areas, such as elasticity, elastoviscoplasticity problems, among others [6]. Cast3M is developed in a specific high level object oriented macro-language – Gibiane – where the solver is integrated with pre-processing and post-processing tools. In the present analysis, the LWAC is assumed as a biphasic medium, composed of mortar ( $m$ ) and LWA ( $a$ ). The compressive behaviour of cylindrical LWAC samples was simulated by assuming, for the sake of simplicity, a plane stress linear isotropic behaviour for both phases.

### 2.2. Reference Experimental Data

Experimental results obtained from a set of LWAC cylindrical samples made of ordinary mortar with 25% of expanded clay 4/10 was taken as benchmark for the present work. The material properties adopted for validation purposes in this study were extracted from reference [5] and are summed in Tab. 1. The aggregate gradation is shown in Tab. 2.

**Table 1.**  
Material's properties [5]

	Description	Value (MPa)
$E_a$	(LWA's Young's modulus )	8030.00
$E_m$	(Mortar's Young's modulus)	28600.00
$f_a$	(LWA's compressive strength)	18.30
$f_m$	(Mortar's compressive strength)	40.20
$p_a$	(LWA's tensile strength)	(*) 2.41
$p_m$	(Mortar's tensile strength)	(**) 8.04
$f_{c,exp}$	(LWAC's compressive strength)	34.00

(\*) This value was obtained from equation (BS EN 13055-1:2003) [4]

$p_a = 3.9 (1.82\rho_{av}/1000 - 0.4)$ , where  $\rho_{av}$  is the bulk density. In the present case,  $\rho_{av} = 560 \text{ kg/m}^3$ ;

(\*\*)  $p_m$  was assumed as 20% of  $f_m$  [7].

**Table 2.**  
Lightweight aggregate gradation.

Sieve Size (mm)	12.5	10.0	8.0	6.3	5.0	4.0	2.5	1.25	pan
% Cumulative Refusal	0	4.68	67.13	85.44	94.84	97.85	99.79	99.94	100

### 2.3. 2D Finite Element Modelling of the LWAC Specimens

The geometry of the 2D models described in this section represents the central longitudinal section of a standard cylindrical sample with 15cm of diameter and 30cm high (BS EN 12390-1:2012) [8], as shown in Fig. 5a and Fig. 5b. The aggregates are considered as spherical, randomly distributed and immerse in mortar, here assumed as a homogenous material. The spheres diameter's distribution reproduce the actual aggregate gradation adopted in the mixture, given in the reference work [5] and presented in Tab. 2.

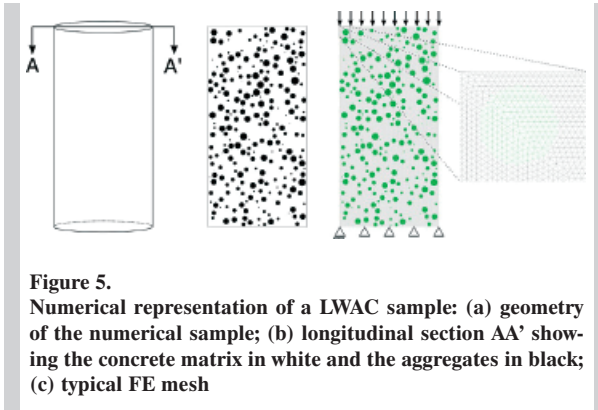


**Figure 5.**  
**Numerical representation of a LWAC sample: (a) geometry of the numerical sample; (b) longitudinal section AA' showing the concrete matrix in white and the aggregates in black; (c) typical FE mesh**

Fig. 5b represents a 2D model of the concrete specimen and the loading and boundary conditions adopted so as to reproduce a compressive test. Fig. 5c illustrates a typical plane stress mesh of linear triangle finite elements, where the two considered phases – mortar and LWA – are clearly identified, as one can see in the detail. In order to account for the dispersion of results, thirty 2D models were generated from the same synthetic sample, each one presenting a different random spatial aggregate distribution.

#### 2.4. Failure Analysis

$E_w$ ,  $f_w$ ,  $E_m$  and  $f_m$  (from Tab. 1) are the input mechanical parameters for the numerical analysis, which consisted of subjecting the modeled concrete specimens to incremental compressive loads (as indicated in Fig. 5c up to failure). The compression stress level of a finite element is defined by means of a quantity named *compression stress level* ( $c_\alpha(i)$ ) where the  $\alpha$  index indicates the phase of the  $i$ -th finite element:  $m$  for mortar and  $a$  for LWA. The  $c_\alpha(i)$  coefficient is evaluated according to Eq. (2):

$$c_\alpha(i) = \frac{\text{abs}(\sigma_2(i))}{f_\alpha} \quad (2)$$

where  $\sigma_2(i)$  is the maximal compressive stress observed in the  $i$ -th element and  $f_\alpha$  is the phase's compressive strength (see Tab. 1). The tensile stress level ( $t_\alpha(i)$ ) is evaluated for every finite element in an analogous manner, as given in Eq. (3):

$$t_\alpha(i) = \frac{\sigma_1(i)}{p_\alpha} \quad (3)$$

where  $\sigma_1(i)$  is the maximal tensile stress in the  $i$ -th finite element and  $p_\alpha$  is the phase's tensile strength (given in Tab. 1). The  $i$ -th element is considered to

reach failure – either under compression or tension – when  $c_\alpha(i)$  and/or  $t_\alpha(i)$  are  $\geq 1$ . It is possible to identify the global failure of a LWAC specimen when a significant amount of finite elements reaches failure. The main goal of the adopted computational procedure is to verify whether the resulting compressive strength numerically obtained approaches its experimental counterpart,  $f_{c,exp} = 34$  MPa (given in Tab. 1).

### 3. NUMERICAL RESULTS

In this preliminary work, the non-linear behaviour observed in actual experiments is not considered. In spite of this fact, the adopted approach showed fair agreement with the reference measurements, as one can see in the following.

In order to verify the convergence of the numerical results, 6 different meshes with increasing refinement levels were adopted to model the 2D concrete sample: M1 (1,832 elements); M2 (11,712 elements); M3 (47,002 elements); M4 (187,874 elements), M5 (293,754 elements) and M6 (423,200 elements). Fig. 6 illustrates the results obtained for the vertical displacement ( $\delta$ ) on the top of the specimen for each adopted mesh ( $M_i$ ) related to that evaluated for mesh M6. As one can see in the figure, results are almost coincident for meshes M4, M5 and M6. Based on this consideration, mesh M4 was adopted for the present analysis.

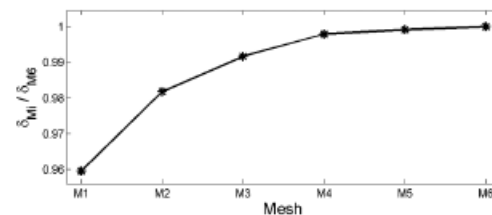


**Figure 6.**  
**Convergence analysis: the curve represents the variation of the vertical displacement on the top of the numerical model for six different FE meshes**

Fig. 7 to Fig. 10 show the amount of failed elements resulting from applied compressive stresses varying from 15 MPa to 34 MPa. The boxplots presented in such figures result from the 30 analyses performed on the numerical specimens, as mentioned in section 2.3. – the red lines standing for the median values. Fig. 7 demonstrates the evolution of the amount of finite elements made of LWA ( $a_{FE}$ ) under compressive failure, indicating that when the concrete sample is under 27 MPa, around 5% of those elements present

$c_a \geq 1$ . That amount reaches about 80% for a compressive loading of 34 MPa. Fig. 9 indicates that for the maximal applied load, there are nearly 10% of a-FE under tensile failure ( $t_a \geq 1$ ). Fig. 8 and Fig. 10 are related to the finite elements composed of mortar ( $m_{FE}$ ). It is seen in Fig. 8 that the amount of  $m_{FE}$  reaching compressive failure varies from 4% – for a 27 MPa loading – to more than 25% under 34 MPa. On the other hand, Fig. 10 shows that there was practically no  $m_{FE}$  under tensile failure ( $c_m \geq 1$ ) for the applied load levels.

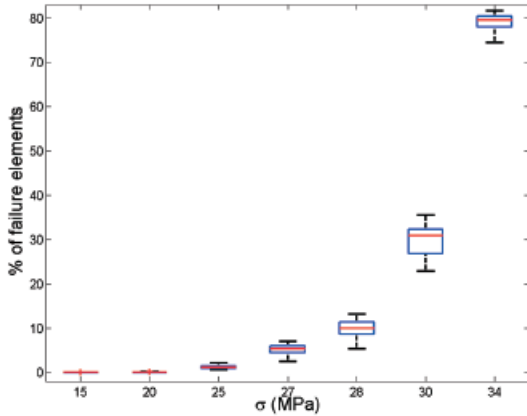


Figure 7. Evolution of the amount of a-FE under compressive failure ( $c_a \geq 1$ )

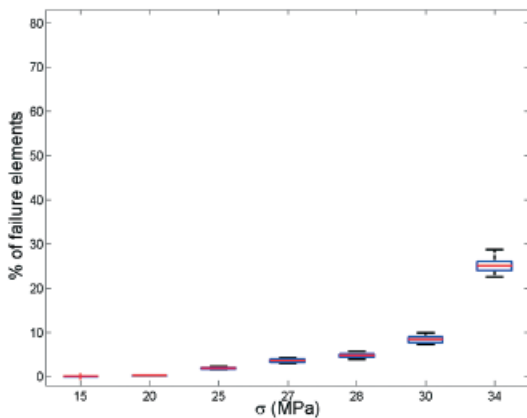


Figure 8. Evolution of the amount of m-FE under compressive failure ( $c_m \geq 1$ )

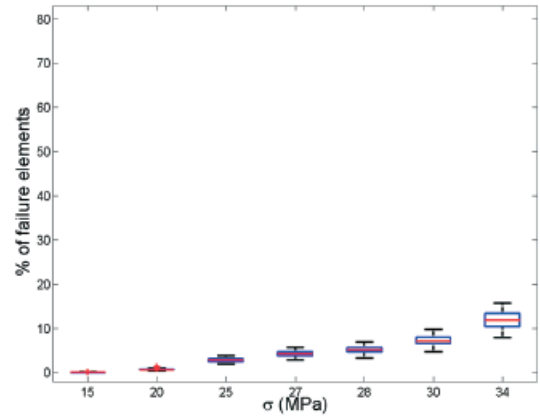


Figure 9. Evolution of the amount of a-FE under tensile failure ( $t_a \geq 1$ )

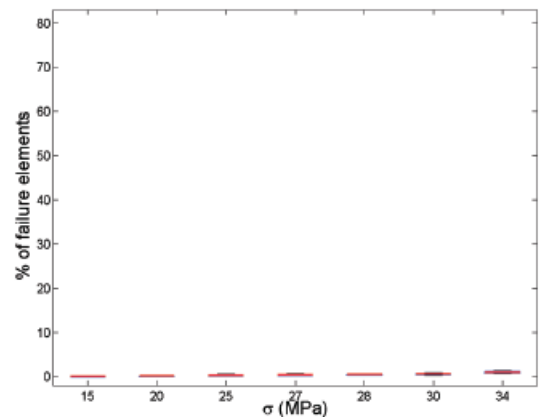


Figure 10. Evolution of the amount of m-FE under tensile failure ( $t_m \geq 1$ )

#### 4. DISCUSSION

In the present analysis, the LWAC sample is considered to reach global failure when a significant amount of finite elements reach their respective stress limits ( $c_a$  and/or  $t_a \geq 1$ ). Fig. 8 to Fig. 10 indicate that such a situation is not observed for loadings up to 27 MPa. From that stage on, an increasing number of finite elements attain failure at each loading step. The numerical result for the LWAC’s compressive strength, though, is estimated as ranging from 27 MPa to 34 MPa. Such a result is considered to fairly agree with the benchmark, of 34 MPa. It is important to notice that the present study does not take into account some specific phenomena that influence the material’s macroscopic behaviour. For instance, the linear mechanical model adopted herein for both the concrete’s components does not reproduce any

stress redistribution resulting from localized failure. This aspect shall be improved by assuming an elasto-plastic non-linear mechanical model, which is expected to increase the global material's strength.

This work is the starting stage of a comprehensive study aiming to apply computational modelling allied to experimental data to the better understanding and prediction of LWAC's behaviour. In spite of the simplifying hypothesis adopted in this stage of the work, the numerical results obtained herein showed fair agreement with their experimental counterpart. This fact encourages further applications with higher complexity related to geometric and mechanical aspects, in order to better reproduce and preview real world problems.

## ACKNOWLEDGEMENTS

Authors thank CNPq (Conselho Nacional de Desenvolvimento Científico e Tecnológico); UFJF (Federal University of Juiz de Fora); FAPEMIG (Fundação de Amparo à Pesquisa do Estado de Minas Gerais) and CAPES (Coordenação de Aperfeiçoamento de Pessoal de Nível Superior) for financial supports.

The paper was presented at the 8<sup>th</sup> International Conference AMCM 2014 – Analytical Models and New Concepts in Concrete and Masonry Structures (AMCM'2014), Wrocław, June 2014.

## REFERENCES

- [1] *Khan Y. S.*; Engineering Architecture: The Vision of Fazlur R. Khan. W.W. Norton & Company, New York, 2004
- [2] *Ke Y. et al.*; Influence of volume fraction and characteristics of lightweight aggregates on the mechanical properties of concrete. Construction and Building Materials, Vol.23, No.8, 2009; p.2821-2828
- [3] GDACE – Group of development and analysis of structural concrete. Development of structural concretes. Available at: <http://www.gdace.uem.br/linhas.htm>. [Accessed 12/03/14]
- [4] BS EN 13055-1: Lightweight aggregate for concrete, mortar and grout. British Standards Institute, London, 2003
- [5] *Ke Y. et al.*; Micro-stress analysis and identification of lightweight aggregate's failure strength by micromechanical modeling. Mechanics of Materials, Vol.68, 2013; p.176-192
- [6] *Le Fichoux E.*; Présentation Et Utilisation De Cast3M. CEA, 2011
- [7] *Rao G. A.*; Generalization of Abram's law for cement mortars. Cement and Concrete Research, Vol.31, No.3, 2001; p.495-502
- [8] BS EN 12390-1: Testing hardened concrete Shape, dimensions and other requirements for specimens and moulds. British Standards Institute, London, 2012